Pulmonary Cryptococcosis: Imaging Findings in 23 Non-AIDS Patients

Kyoung Doo Song, MD[1]
Kyung Soo Lee, MD[1]
Man Pyo Chung, MD[2]
O Jung Kwon, MD[2]
Tae Sung Kim, MD[1]
Chin A Yi, MD[1]
Myung Jin Chung, MD[1]

Index terms:
Cryptococcosis
Lung, infection
Lung, CT
PET

DOI:10.3348/kjr.2010.11.4.407

Korean J Radiol 2010;11:407-416
Received December 28, 2009; accepted after revision February 16, 2010.

[1]Department of Radiology and Center for Imaging Science; [2]Division of Pulmonary and Critical Care Medicine at the Department of Internal Medicine, Samsung Medical Center, Sungkyunkwan University School of Medicine, Seoul 135-710, Korea

This work was supported by the Korea Science and Engineering Foundation (KOSEF) grant funded by the Korea government (MEST) (R11-2002-103).

Address reprint requests to:
Kyung Soo Lee, MD, Department of Radiology, Samsung Medical Center, Sungkyunkwan University School of Medicine, 50 Ilwon-dong, Gangnam-gu, Seoul 135-710, Korea.
Tel. (822) 3410-2518
Fax. (822) 3410-2559
e-mail: kyungs.lee@samsung.com

Objective: We aimed to review the patterns of lung abnormalities of pulmonary cryptococcosis on CT images, position emission tomography (PET) findings of the disease, and the response of lung abnormalities to the therapies in non-AIDS patients.

Materials and Methods: We evaluated the initial CT (n = 23) and 18F-fluorodeoxyglucose (FDG) PET (n = 10), and follow-up (n = 23) imaging findings of pulmonary cryptococcosis in 23 non-AIDS patients. Lung lesions were classified into five patterns at CT: single nodular, multiple clustered nodular, multiple scattered nodular, mass-like, and bronchopneumonic patterns. The CT pattern analyses, PET findings, and therapeutic responses were recorded.

Results: A clustered nodular pattern was the most prevalent and was observed in 10 (43%) patients. This pattern was followed by solitary pulmonary nodular (n = 4, 17%), scattered nodular (n = 3, 13%), bronchopneumonic (n = 2, 9%), and single mass (n = 1, 4%) patterns. On PET scans, six (60%) of 10 patients showed higher FDG uptake and four (40%) demonstrated lower FDG uptake than the mediastinal blood pool. With specific treatment of the disease, a complete clearance of lung abnormalities was noted in 15 patients, whereas a partial response was noted in seven patients. In one patient where treatment was not performed, the disease showed progression.

Conclusion: Pulmonary cryptococcosis most commonly appears as clustered nodules and is a slowly progressive and slowly resolving pulmonary infection. In two-thirds of patients, lung lesions show high FDG uptake, thus simulating a possible malignant condition.

Cryptococcus neoformans is a ubiquitous encapsulated yeast-like fungus that is found worldwide; particularly in soils that are contaminated with pigeon excreta and decayed wood (1–3). Inhalation of cryptococcal particles into the lungs is a route of pulmonary infection, and subsequent hematogenous dissemination may cause central nervous system infection (1). Cryptococcal infections are mostly common in immunocompromized patients such as those with AIDS, who underwent organ transplantation, or who have a hematologic malignancy. These infections are relatively rare in immunocompetent patients (2).

Pulmonary cryptococcosis in AIDS patients tends to manifest itself as a disseminated thoracic disease with an interstitial lung pattern and lymph node enlargement as seen on imaging studies (4–8); whereas the infection in immunocompetent hosts shows single or multiple nodular lesions or mass-like consolidation (8–11). The infection in non-AIDS patients is rather indolent in nature and is usually not treated systemically when the disease appears as a localized nodular or a consolidative lesion (12).

Therefore, lung lesions of single or multiple nodules or a mass, for this condition, may persist and may simulate malignant disease, a chronic inflammatory or an infectious disease, or a metastatic lesion, particularly when patients have an underlying extra-thoracic malignancy.

Different treatment options have been advocated for this infection in non-AIDS patients including surgical resection, antifungal treatment, or observation without specific treatment (12, 13). However, the natural course of the disease on imaging studies, particularly how quickly the lung lesions evolve before adequate treatment of the disease and how the lung lesions show response to surgical or antifungal therapy, has not been well documented. Only a few reports document the PET findings of pulmonary cryptococcosis (14–17). Thus, the purpose of our study was to review patterns of lung abnormalities of pulmonary cryptococcosis on CT images, assess the PET findings of the disease, and evaluate the response of lung abnormalities to the different therapies.

MATERIALS AND METHODS

Our Institutional Review Board approved our retrospective study with a waiver of the informed consent from each patient.

Patients

This was a retrospective study for patients with pulmonary cryptococcal infection who were seen in a single tertiary-referral hospital over the course of a 14-year period (January 1995 to December 2008) and who underwent thoracic CT examinations. By using the electronic database of medical records, we could identify 23 patients, who had histopathologically-proven pulmonary cryptococcosis. Over the same span of time, we could not find any patient who had AIDS and cryptococcal infection. The patient population consisted of 13 men and 10 women, with an age range from 32 years to 77 years (median, 57 years; mean age $\pm$ standard deviation [SD], 56 $\pm$ 12.4 years). None of the patients showed central nervous system involvement for the disease.

If a patient had at least one of the following conditions: underlying malignancy, use of immunosuppressive drugs, uncontrolled diabetes mellitus, or liver cirrhosis, the patient was considered to be immunocompromised. Even though a patient had a history of malignancy, the patient was considered to be immunocompetent when he or she was in a disease-free state for more than five years. Thirteen patients had various underlying diseases including breast cancer in three patients, hepatocellular carcinoma in two patients, as well as colon cancer, cholangiocellular carcinoma, renal cell carcinoma, pancreatic cancer, diffuse large B-cell lymphoma, advanced gastric cancer, esophageal cancer, and herpes simplex encephalitis in one patient each. Of the 12 patients with an underlying malignancy, three patients were in a disease-free state for more than five years. However, one of the three patients in the disease-free state had liver cirrhosis. Thus, this patient was classified as immunocompromised. As a result, 11 (10 patients with an underlying malignancy and one with herpex simplex encephalitis) patients were considered to be immunocompromised and 12 patients were considered to be immunocompetent (Table 1).

The diagnosis of the pulmonary fungal infection was made with the aid of histopathological specimens. The specimens were obtained via a percutaneous gun (core) biopsy for lung lesions in eight patients, a wedge resection using video-assisted thoracoscopic surgery (VATS) in 13 patients, and a right middle lobectomy performed by way of VATS or wedge resection after an open thoracotomy, respectively for one patient for each method. The histopathological diagnoses were rendered by identifying encapsulated yeast forms within inflammatory lung tissue with the use of Hematoxylin and eosin, mucicarmine, periodic acid-Schiff, or Gomori-methenamin-silver staining. A serum cryptococcal antigen test demonstrated positivity in only three (21%) of 14 patients in which the test was performed.

Patient Demographics

The symptoms or signs of patients, if any, were recorded. In addition, clinicoradiological diagnoses before the definitive diagnosis of cryptococcosis were recorded. Eleven patients had previously undergone CT scans (scan interval; range = 1 – 75 days, median time = 18 days, mean time = 21.7 days) that had been obtained at outside institutions. PET (n = 1) or PET/CT (n = 9) scans were available for 10 patients.

Image Acquisition and Interpretation

Helical Enhanced CT Imaging

All chest CT examinations for patients at the time of presentation were performed using a single-detector (two patients; HiSpeed Advantage scanner, GE Healthcare, Milwaukee, WI), 4-detector (eight patients; LightSpeed QX/I, GE Healthcare), 8-detector (five patients; LightSpeed Ultra, GE Healthcare), 16-detector (four patients; LightSpeed Ultra or Ultra16, GE Healthcare), or 64-detector (four patients; LightSpeed VCT XT, GE Healthcare) row scanners. Helical CT scans (125–200 mA, 120 kVp; 5-mm section thickness and a pitch of 1 for single-detector helical CT and beam width of 10–20 mm,

beam pitch of 1.375–1.5 for multidetector CT) were obtained from the lung apices to the level of the middle portion of both kidneys after an intravenous contrast medium injection of 80 mL Iomeron 300 (Iomeprol; Bracco, Milan, Italy). The image data were reconstructed with a high-spatial algorithm for lung window images, a standard algorithm for mediastinal window images, a 5-mm section thickness for single-detector helical CT scans, and with a 2.5-mm section thickness for multidetector CT scans. All image data were directly interfaced with a picture archiving and communication systems (PACS) (PathSpeed, or Centricity 2.0; GE Healthcare, Mt. ProSpect, IL), which displayed all image data on two monitors (1,536 × 2,048 matrix, 8-bit viewable gray scale, and 60-ft-Lambert luminescence). Both mediastinal (width, 400 HU; level, 20 HU) and lung (width, 1,500 HU; level, −700 HU) window images were viewed on these monitors.

Scans were assessed for the presence of lung abnormalities (nodules, masses, consolidation, and ground-glass opacity) and distribution (laterality and lobar location, lingular division was classified as a separate lobe) at the time of presentation. Two chest radiologists performed the evaluations and decisions on the findings that were reached by consensus. Nodules were defined as round or oval opacities with at least moderately well circumscribed margins that had a maximum diameter of 3 cm or less. If a rim of ground-glass opacity surrounded a nodule, the halo sign was considered present. When opacities were greater than 3 cm in diameter, the lesions were defined as masses. The criteria for consolidation were met when parenchymal non-nodular opacity obscured the underlying pulmonary architecture and often accompanied air bronchograms. Ground-glass opacity was defined as hazy opacities through which the normal pulmonary architecture could be visualized. The presence of cavitation within nodules or masses was noted. The presence of pleural effusion and lymphadenopathy (when the short-axis diameter was greater than 10 mm) were also recorded.

After the assessment of lung parenchymal abnormalities, the lung lesions were further classified into five patterns: single nodular, multiple clustered nodular, multiple

Table 1. Demographic and Clinical Information of Patients

Patients	Age/Sex	Presenting Symptom	Immune Status/ Underlying Disease	Radiologic Diagnosis before Biopsy	Treatment Regimen (months)
1	32/M	No	Competent/No	Tuberculosis	WR
2	58/M	No	Competent/No	Tuberculosis	WR
3	35/F	Cough, fever	Competent/No	Tuberculosis	Fluconazole, 12
4	64/F	No	Competent/No	Lung cancer	WR
5	53/M	Chest pain	Competent/No	Tuberculosis	WR
6	40/M	Chest pain	Competent/No	Lung cancer	Lobectomy + Fluconazole, 2
7	38/M	Cough and chest pain	Competent/No	Tuberculosis	Fluconazole, 4
8	52/F	Cough and sputum	Competent/No	Lung cancer	Fluconazole, 12
9	51/M	Chest pain	Competent/No	Tuberculosis	Fluconazole, 4
10	41/F	Cough	Competent/No	Tuberculosis	Fluconazole, 6
11	53/M	No	Competent/HCC NED	Tuberculosis	No
12	68/F	No	Competent/Breast cancer NED	Metastasis	WR + Fluconazole, 6
13	71/F	Cough	Compromised/AGC	Metastasis	WR + Fluconazole, 6
14	57/F	No	Compromised/Breast cancer	Metastasis	WR + Fluconazole, 5
15	70/F	No	Compromised/RCC	Metastasis	WR
16	63/M	No	Compromised/CCC	Tuberculosis	WR
17	49/M	No	Compromised/Pancreatic cancer, DM	Paragonimiasis	Fluconazole, 4
18	77/F	Cough and sputum	Compromised/DLBL	Lymphoma involvement	WR + Fluconazole, 4
19	58/M	No	Compromised/Esophageal cancer	Metastasis	WR
20	65/M	No	Compromised/HCC NED, LC	OP	WR+ Fluconazole , 2
21	50/M	No	Compromised/Colon cancer	Metastasis	WR
22	72/F	No	Compromised/Breast cancer	OP	WR + Fluconazole, 4
23	61/M	Fever	Compromised/Herpes simplex encephalitis	Cryptococcosis	Amphotericin B, 19 days and Fluconazole, 4

Note.— AGC = advanced gastric cancer, CCC = cholangiocellular carcinoma, DLBL = diffuse large B-cell lymphoma, DM = diabetes mellitus, HCC = hepatocellular carcinoma, LC = liver cirrhosis, NED = no evidence of disease, OP = organizing pneumonia, RCC = renal cell carcinoma, WR = wedge resection

scattered nodular, mass-like, and bronchopneumonic patterns. Single nodular and mass-like patterns were defined when the lung lesion consisted of a single nodule and a single mass, respectively. The multiple clustered nodular pattern was defined when the lesions consisted of multiple variable-sized nodules confined to one lobe, whereas the multiple scattered nodular pattern was defined when lesions consisted of multiple variable-sized nodules scattered throughout multiple lobes in a single lung or in both lungs. The bronchopneumonic pattern was defined as when lung lesions were comprised of areas of lobular, subsegmental, or segmental consolidation, ill-defined centrilobular small nodules (measuring 4 to 10 mm in diameter and representing peribronchiolar consolidation) or tree-in-bud (small centrilobular nodules and branching nodules within the secondary pulmonary lobule) opacities (18). When lung lesions could not be classified into one of the five patterns, they were classified as unclassifiable.

In 11 patients, where previous CT scans were available, the scans were also analyzed with the use of the above-mentioned methods and the findings were compared with those seen on CT scans at the time of presentation.

PET or PET/CT

Details on imaging methods have been described in previous reports (19, 20). Briefly, the peripheral blood glucose levels were $\leq$ 150 mg/dL in all patients. Patients received an intravenous injection of 370 MBq (10 mCi) 18F-fluorodeoxyglucose (FDG) and were then allowed to rest for over 45 minutes prior to scanning. Image acquisition was achieved by way of a PET (Advance, GE Healthcare, Milwaukee, WI) or PET/CT device (Discovery LS, GE Healthcare) consisting of an Advance NXi PET scanner and an 8-slice LightSpeed Plus CT scanner.

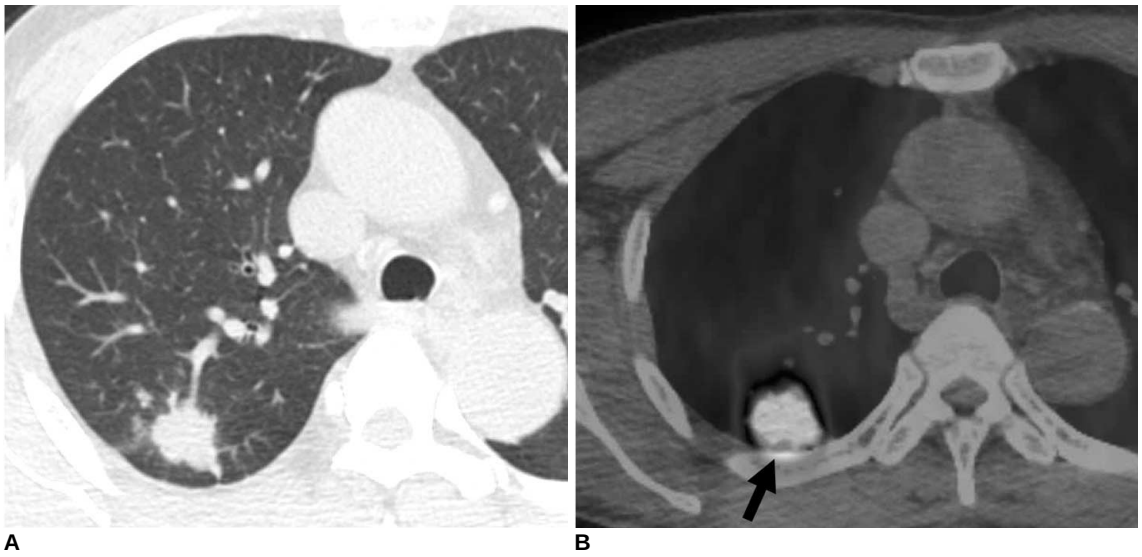

Fig. 1. Pulmonary cryptococcosis with clustered nodular pattern in 53-year-old man who had hepatocellular carcinoma (patient 11 in Tables 1, 2).
A. Lung window of transverse CT scan obtained at level of distal trachea demonstrates clustered nodules in posterior segment of right upper lobe.
B. PET/CT scan obtained at similar level to **A** demonstrates high FDG uptake (arrow) within main nodule (maximum standardized uptake value, 9.3), hence simulating malignant nodule.
C. Follow-up CT scan obtained at similar level to and three months after **A** demonstrates slightly increased extent of clustered nodules in right upper lobe.

PET or PET/CT examinations were performed as part of a metastatic workup in six patients because these patients had extra-thoracic malignant disease. In the remaining four patients, studies were performed for nodule characterization.

Integrated PET/CT images were evaluated by a nuclear medicine physician who was unaware of the clinical or histopathological findings. The maximum FDG standardized uptake value (mSUV) of lung lesions was measured for the lung abnormalities.

Treatment and Follow-Up Imaging Studies

The treatments administered were as follows: no specific treatment after the diagnosis of pulmonary cryptococcosis in one patient; surgical resection only for both diagnosis and treatment as well as the use of VATS or open thoracotomy in eight patients; antifungal therapy (Fluconazole; Plunazole, Daewoong Pharm, Seoul, Korea) following a diagnostic lung lesion resection in seven patients. The remaining seven patients underwent antifungal therapy after a diagnostic core biopsy. The mean treatment duration of antifungal therapy in 14 patients was five months (range, 2–12 months).

Follow-up imaging studies (with CT in 16 patients and with chest radiographs in seven patients) were obtained for all patients. The follow-up period ranged from two to 26 months (median, 7 months; mean, 9 months). Responses on imaging studies were classified into partial, complete, or no response.

RESULTS

Of the 23 patients, 13 (57%) had no symptoms or signs. In 10 (43%) patients, symptoms including cough (n = 6), chest pain (n = 4), sputum (n = 2), and fever (n = 2) were observed. Before the definitive diagnoses of cryptococcosis had been determined, clinicoradiological diagnoses for the disease included pulmonary tuberculosis (n = 9), metastases from an extra-thoracic malignancy (n = 6), lung cancer (n = 3), organizing pneumonia (n = 2), pulmonary paragonimiasis (n = 1), lymphomatous involvement of the lung (n = 1), and pulmonary cryptococcosis (n = 1) (Table 1).

Lesion Evolvement Depicted on CT Imaging

Of the 11 patients who had undergone previous CT scans (nine of the 11 patients received empirical antibiotic treatment based on the assumption that the patients had community acquired pneumonia), seven (67%) showed a progression of the same pattern of disease, whereas four (33%) showed no change in the extent of the disease. None of the patients showed improvement in the course of the disease (Table 2). Of the nine patients, whose largest lesion's maximum diameter was measurable in both previous and current CT scans, seven patients showed no change in the maximum diameter of the lesion within a 34 day follow-up period, however two patients demonstrated an interval increase (2.5 and 2.6 times) in lesion diameters over 50 and 75 day follow-up period, respectively.

CT Findings

A clustered nodular pattern (Fig. 1) of lung abnormalities was the most frequent pattern and was observed in 10 (43%) patients. A solitary pulmonary nodular pattern (n = 4, 17%) (Fig. 2) and scattered nodular pattern (n = 3, 13%) (Fig. 3) were the next most common patterns for lung lesions. A bronchopneumonic pattern (Fig. 4) was noted in two (9%) patients, and a single mass lesion (Fig. 5) was identified in one patient (4%). In three patients, lung lesions were unclassifiable: one patient had a mass and a nodule, another patient had an area of consolidation and multiple scattered nodules in the left lung, and the third patient had clustered masses and nodules in the bilateral lower lung zones (Table 2).

In immunocompetent patients (n = 12), a clustered nodular pattern (n = 6, 50%), scattered nodular pattern (n = 2, 17%), solitary pulmonary nodular pattern (n = 1, 8%), solitary mass (n = 1, 8%), and unclassifiable lesions (n = 2, 16%) were observed. In immunocompromised patients (n = 11), a clustered nodular pattern (n = 4, 36%), solitary pulmonary nodular pattern (n = 3, 27%), bronchopneumonia pattern (n = 2, 18%), scattered

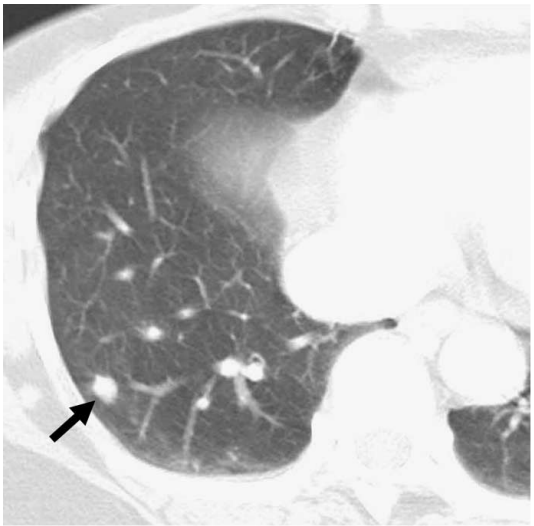

Fig. 2. Pulmonary cryptococcosis of solitary pulmonary nodular pattern in 58-year-old man who had esophageal cancer (patient 19 in Tables 1, 2). Lung window of transverse CT scan obtained at level of suprahepatic inferior vena cava shows 7-mm-sized solitary pulmonary nodule (arrow) in right lower lobe.

nodular pattern (n = 1), and unclassifiable lesions (n = 1, 9%) were observed.

Of the six lobes observed (lingular division was considered as a separate lobe), the left lower lobe was most frequently involved (nine cases). The right lower lobe was involved in seven cases, the left upper lobe and the lingular division were involved in six cases each, the right middle lobe was involved in five cases, and the right upper lobe was involved in four cases.

Cavitation within lung parenchymal lesions was noted in four (17%) patients. A nodule with a halo sign was also observed in two (9%) patients. Mediastinal lymph node enlargement was not noted in any patient. Pleural effusion was noted in one (4%) patient, but pericardial effusion was not observed in any patient.

PET Findings

Of the 10 patients that underwent PET, six showed higher FDG uptake compared to the mediastinal blood pool, thus simulating malignant FDG uptake, whereas four patients demonstrated a benign type of FDG uptake. The mSUVs for FDG uptake of lung parenchymal lesions

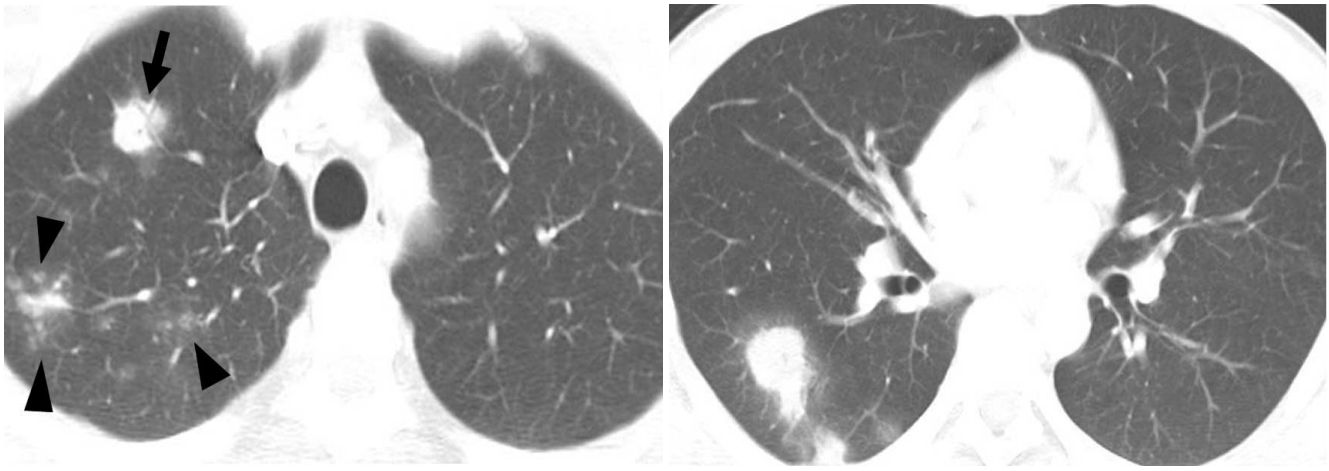

A **B**

Fig. 3. Pulmonary cryptococcosis with scattered nodular pattern in 38-year-old man who had no underlying disease (patient 7 in Tables 1, 2).
A. Lung window of transverse CT scan obtained at level of great vessels shows nodule (arrow) with surrounding ground-glass opacity (halo sign) and centrilobular small nodules (arrowheads) in right upper lobe.
B. CT scan obtained at level of basal trunk demonstrates nodules with halo sign in superior segment of right lower lobe.

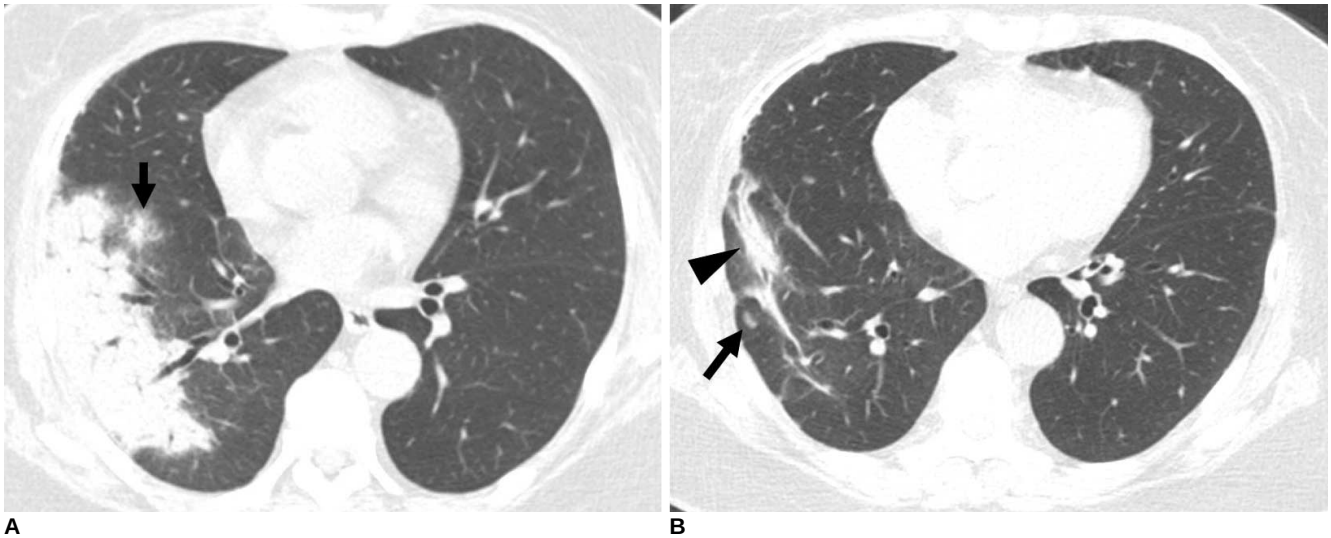

A **B**

Fig. 4. Cryptococcosis of bronchopneumonic pattern in 72-year-old woman who has underlying breast cancer (patient 22 in Tables 1, 2).
A. Lung window of transverse CT scan obtained at level of right inferior pulmonary vein shows subpleural consolidation and nodule (arrow) with surrounding halo in right lower lobe.
B. Follow-up CT scan obtained five months after **A** and with four months of anti-fungal therapy demonstrates remaining lesions of consolidation (arrowhead) and nodule (arrow) in right lower lobe.

ranged from 1.8 to 9.3 (median, 5.3; mean, 5.4) (Table 2).

Follow-Up Study

No patient died from the pulmonary cryptococcosis. Clinical or radiological improvement was identified in 22 (96%) patients. In one patient (4%) with underlying hepatocellular carcinoma and no specific treatment was given, the parenchymal lesions of clustered nodules showed disease progression over a five-month follow-up period (Fig. 1).

Of the 22 patients treated, complete clearance of lung abnormalities was noted in 15 (65%) patients including four patients who had solitary pulmonary nodular lesions. In one patient, lesions disappeared completely with antifungal therapy only (patient 23 in Tables 1, 2). Fourteen (93%) of the 15 patients with complete clearance underwent surgical resection for the diagnostic workup. In nine (64%) of the 14 patients, lesions were relatively localized (clustered nodules, solitary pulmonary nodule, or a mass and a nodule). Therefore, a diagnostic surgical resection removed all lesions. After the surgical resection, new nodular lesions developed in one patient (patient 14 in Tables 1, 2) on follow-up CT scans obtained two months later. This patient was treated with antifungal agents for five months and the new lesions disappeared after the treatment. In the remaining eight patients, there was no newly developed lesion on follow-up scans. In another five (36%) patients, diagnostic surgical resection could not remove all lesions. Thus, additional antifungal therapy was administered. Therefore, a total of six patients, where complete lesion clearance was achieved, received antifungal therapy after the surgical resection. In these six patients, the mean treatment duration was 4.2 months (range, 2–6 months).

In seven (31%) patients, although improvement of lung lesions with a decreased extent of abnormalities was observed, the remaining lung lesions persisted (partial response) during the median follow-up period of 11 months (range, 5–26 months; mean, 13 months) (Fig. 4) (Table 2).

Table 2. Imaging Findings of Cryptococcosis in 23 Patients

Patients	Previous CT Patterns (mm)	Follow-Up Interval (days)	CT Findings at Presentation			PET Findings (mSUV)	Follow-Up CT or CXR Findings	Follow-Up (months)
			Main Patterns (mm)*	Laterality	Predominant Zone/ Location			
1	CNs (6)	50	CNs (15)	U	LLL	2.9	CR	2
2	CNs (17)	12	CNs (17)	U	RLL	2.8	CR	4
3	–	–	CNs (28)	U	LLL	–	PR	26
4	–	–	CNs (16)	U	Lingular	–	CR	11
5	CNs (20)	8	CNs (20)	U	RLL	2.0	CR on CXR	12
6	SPN (17)	7	SPN (17)	U	RML	7.9	CR	4
7	SNs (25)	13	SNs (28)	B	Both lungs	–	PR on CXR	5
8	–	–	Solitary mass (44)	U	RML	–	PR	11
9	SNs (27) + consolidation	3	SNs (28) + consolidation	U	Left lung	–	PR on CXR	21
10	Clustered masses and nodules	18	Clustered masses (60) and nodules	U	LLL	–	PR	12
11	–	–	CNs (20)	U	RUL	9.3	Slight progression	5
12	SNs (5)	75	SNs (13)	B	Both lungs	8.8	CR on CXR	7
13	–	–	CNs (15)	U	LUL	–	CR on CXR	5
14	–	–	SPN (10)	U	RLL	1.8	CR	7
15	–	–	A mass (38) + a nodule (16)	U	LUL	–	CR	6
16	CNs (15)	1	CNs (15)	U	LLL	4.8	CR	15
17	–	–	CNs (14)	U	RML	–	PR	10
18	–	–	CNs (12)	U	Lingular	7.2	CR on CXR	11
19	–	–	SPN (7)	U	RLL	–	CR	3
20	SNs (19)	34	SNs (21)	U	LLZ	5.7	CR	10
21	–	–	SPN (8)	U	RUL	–	CR on CXR	6
22	Bronchopneumonia	18	Bronchopneumonia	U	RLL	–	PR	8
23	–	–	Bronchopneumonia	U	Left lung	–	CR	5

Note.— * maximum diameter (of largest lesion), B = bilateral, CNs = clustered nodules, CR = complete remission, CXR = chest radiograph, LLL = left lower lobe, LLZ = lower lung zone, LUL = left upper lobe, mSUV = maximum standardized uptake value, - = not available, PR = partial remission, RLL = right lower lobe, RML = right middle lobe, RUL = right upper lobe, SNs = scattered nodules, SPN = solitary pulmonary nodule, U = unilateral

Fig. 5. Pulmonary cryptococcosis of solitary mass pattern in 52-year-old woman with no underlying disease (patient 8 in Tables 1, 2). Lung window of CT scan obtained at level of right middle lobar bronchus shows mass in right middle lobe.

Of seven patients who were treated with antifungal agents only, one patient (patient 23 in Tables 1, 2, treated with amphotericin and fluconazole) showed complete clearance. In the remaining six patients, who were treated with fluconazole, a partial response was noted. The mean follow-up period was 14 months (range, 5–26 months). In these six patients with remaining disease, symptoms such as a cough, sputum, fever, and chest pain disappeared within three or six months of the treatment outset.

DISCUSSION

In our study, the most frequent pattern of lung abnormalities depicted on CT scans was clustered nodules, which was observed in 10 (43%) patients. This pattern was followed by solitary pulmonary nodular (n = 4, 17%) and scattered nodular (n = 3, 13%) patterns. Thus, nodular lesions localized to a lobe or scattered to lung(s) accounted for 73% of lung parenchymal abnormalities. Our results concur with findings of previous reports in which clustered nodules or a solitary pulmonary nodule was the most common pattern of lung abnormalities for pulmonary cryptococcosis (9–11, 21).

Of the 11 patients that underwent previous CT scans before presentation, all patients showed slow progression or no change with respect to the extent of the lung lesions. In particular, two patients, in which the lesions increased in size by more than two times the original diameter at approximately 50 days after the initial assessment. None of the patients showed spontaneous resolution of parenchymal lung lesions. Therefore, a specific diagnosis of cryptococcosis is mandatory for the management of this infection. On the other hand, the chronicity of lung lesions was noted after the diagnosis of the disease was confirmed. Lung lesions were indolent and the lung lesions did not show a rapid response to antifungal therapy.

In our study, 11 (48%) of 23 patients were immunocompromised and 12 were immunocompetent. However, the disease patterns between the two groups were not different. Furthermore, none of the immunocompromised patients showed a disseminated disease pattern such as diffuse interstitial lung disease accompanied by extensive hilar and mediastinal lymphadenopathy.

It is well known that active tuberculosis or tuberculoma, acute and chronic pneumonia, lung abscess, fungal infection, and parasitic infestation are frequent causes of increased FDG uptake (22). For these conditions, the presence and activity of leukocytes account for the increased FDG uptake. Activated macrophages and neutrophils in inflammatory tissue utilize glucose as an energy source for chemotaxis and phagocytosis, whereas fibroblasts utilize glucose for proliferation. In our study, six (60%) of 10 patients that underwent PET or PET/CT scans showed high FDG uptake. Moreover, five (83%) of these six patients had an underlying malignancy. Pulmonary metastases could not be excluded in these five patients because of the presence of multiple pulmonary nodules with a high rate of FDG uptake were noted on the PET scans, even though the nodules showed clustering on CT scans, persisted for a quite amount of time. Thus, even in patients with an underlying malignancy and lung nodules that demonstrate high FDG uptake, when nodules are clustered in a lobe, a histopathological diagnosis should be performed for tissue confirmation.

The complete clearance of lung abnormalities was achieved in 15 patients. Of these 15 patients, surgical resection with or without subsequent antifungal therapy was needed for complete clearance in 14 patients. In the remaining patient, complete clearance was achieved with antifungal therapy only. In the seven patients that were administered antifungal therapy only, a partial response was noted in six patients. In these six patients, although clinical improvement was achieved, the lung lesions persisted after the treatment, as seen on serial imaging studies. In one patient that was not given a treatment, the disease showed progression. Thus, lung lesions were indolent and they did not show a rapid response to antifungal therapy.

Actinomycosis, semi-invasive aspergillosis, and pulmonary tuberculosis are well-known representative causes of chronic pneumonias that usually show an indolent disease course, before and after treatment. These three diseases usually present as single or multiple nodule(s) or mass or as a single area of dense consolidation

(23–25). Therefore, for chronic indolent lung lesions of various patterns including pulmonary cryptococcosis, tuberculosis, actinomycosis, and semi-invasive aspergillosis should be considered for the differential diagnosis of chronic pneumonia.

Our study has several limitations; first, our study was retrospective by design. A prospective study on the imaging diagnosis or treatment method should be performed. Second, there is a possibility that selection bias may have occurred. This is apparent as 12 of 23 patients had an underlying malignancy. Moreover, all 23 patients had biopsy-proven disease. More mild disease may have evaded our patient selection. Third, because of the limited number of patients with the disease, diverse CT findings of the disease and variable follow-up periods, we were not able to provide meaningful CT data or findings that help predict patient prognosis (complete disappearance versus remaining disease).

In conclusion, pulmonary cryptococcosis is an indolent lung disease in non-AIDS patients that is slowly progressive in nature, even without adequate treatment. Moreover, it does not show a rapid resolution of the lung abnormalities even with antifungal therapy. The disease may appear with various patterns of lung lesions; however, a multiple clustered-nodular pattern, localized to a lung lobe, is the most common abnormality. In half of the cases, the disease appeared in patients with underlying disease, in which most of the patients have an extra-thoracic malignant condition. Therefore, when lung lesions show clustered or scattered nodules of an indolent nature, pulmonary cryptococcosis should be considered in the differential diagnosis, even for a patient with an extra-thoracic malignancy. The lesions may show high FDG uptake and may thus simulate a malignant lung condition at PET. Although clinical improvement can be achieved in all patients, radiological improvement is slow, even after antifungal therapy. Lastly, lung lesions may persist for a long time, showing a divergence from the clinical response.

References

1. Sarosi GA. Cryptococcal pneumonia. *Semin Respir Infect* 1997;12:50-53
2. Woodring JH, Ciporkin G, Lee C, Worm B, Woolley S. Pulmonary cryptococcosis. *Semin Roentgenol* 1996;31:67-75
3. Levitz SM. The ecology of Cryptococcus neoformans and the epidemiology of cryptococcosis. *Rev Infect Dis* 1991;13:1163-1169
4. Miller WT Jr, Edelman JM, Miller WT. Cryptococcal pulmonary infection in patients with AIDS: radiographic appearance. *Radiology* 1990;175:725-728
5. Meyohas MC, Roux P, Bollens D, Chouaid C, Rozenbaum W, Meynard JL, et al. Pulmonary cryptococcosis: localized and disseminated infections in 27 patients with AIDS. *Clin Infect Dis* 1995;21:628-633
6. Friedman EP, Miller RF, Severn A, Williams IG, Shaw PJ. Cryptococcal pneumonia in patients with the acquired immunodeficiency syndrome. *Clin Radiol* 1995;50:756-760
7. Lacomis JM, Costello P, Vilchez R, Kusne S. The radiology of pulmonary cryptococcosis in a tertiary medical center. *J Thorac Imaging* 2001;16:139-148
8. Khoury MB, Godwin JD, Ravin CE, Gallis HA, Halvorsen RA, Putman CE. Thoracic cryptococcosis: immunologic competence and radiologic appearance. *AJR Am J Roentgenol* 1984;142:893-896
9. Zinck SE, Leung AN, Frost M, Berry GJ, Müller NL. Pulmonary cryptococcosis: CT and pathologic findings. *J Comput Assist Tomogr* 2002;26:330-334
10. Fox DL, Müller NL. Pulmonary cryptococcosis in immunocompetent patients: CT findings in 12 patients. *AJR Am J Roentgenol* 2005;185:622-626
11. Lindell RM, Hartman TE, Nadrous HF, Ryu JH. Pulmonary cryptococcosis: CT findings in immunocompetent patients. *Radiology* 2005;236:326-331
12. Aberg JA, Mundy LM, Powderly WG. Pulmonary cryptococcosis in patients without HIV infection. *Chest* 1999;115:734-740
13. Nadrous HF, Antonios VS, Terrell CL, Ryu JH. Pulmonary cryptococcosis in nonimmunocompromised patients. *Chest* 2003;124:2143-2147
14. Huang CJ, You DL, Lee PI, Hsu LH, Liu CC, Shih CS, et al. Characteristics of integrated 18F-FDG PET/CT in pulmonary cryptococcosis. *Acta Radiol* 2009;50:374-378
15. Vinson AE, Solis V, Williams HT, Bell B. F-18-FDG-PET/CT leads to diagnosis of cryptococcal pneumonia where recurrent metastatic rhabdomyosarcoma was suspected. *Clin Nucl Med* 2007;32:401-403
16. Igai H, Gotoh M, Yokomise H. Computed tomography (CT) and positron emission tomography with [18f]fluoro-2-deoxy-D-glucose (FDG-PET) images of pulmonary cryptococcosis mimicking lung cancer. *Eur J Cardiothorac Surg* 2006;30:837-839
17. Hsu CH, Lee CM, Wang FC, Lin YH. F-18 fluorodeoxyglucose positron emission tomography in pulmonary cryptococcoma. *Clin Nucl Med* 2003;28:791-793
18. Webb WR, Muller NL, Naidich DP. *High-resolution CT of the lung*, 4th ed. Philadelphia: Lippincott Williams & Wilkins, PA 2009
19. Shim SS, Lee KS, Kim BT, Chung MJ, Lee EJ, Han J, et al. Non-small cell lung cancer: prospective comparison of integrated FDG PET/CT and CT alone for preoperative staging. *Radiology* 2005;246:1011-1019
20. Kim YK, Lee KS, Kim BT, Choi JY, Kim H, Kwon OJ, et al. Mediastinal nodal staging of nonsmall cell lung cancer using integrated 18F-FDG PET/CT in a tuberculosis-endemic country: diagnostic efficacy in 674 patients. *Cancer* 2007;109:1068-1077
21. Chang WC, Tzao C, Hsu HH, Lee SC, Huang KL, Tung HJ, et al. Pulmonary cryptococcosis: comparison of clinical and radiographic characteristics in immunocompetent and immunocompromised patients. *Chest* 2006;129:333-340
22. Shim SS, Lee KS, Kim BT, Choi JY, Chung MJ, Lee EJ. Focal parenchymal lung lesions showing a potential of false-positive and false-negative interpretations on integrated PET/CT. *AJR Am J Roentgenol* 2006;186:639-648
23. Cheon JE, Im JG, Kim MY, Lee JS, Choi GM, Yeon KM. Thoracic actinomycosis: CT findings. *Radiology* 1998;209:229-

233
24. Aquino SL, Kee ST, Warnock ML, Gamsu G. Pulmonary aspergillosis: imaging findings with pathologic correlation. *AJR Am J Roentgenol* 1994;163:811-815
25. Kim SY, Lee KS, Han J, Kim J, Kim TS, Choo SW, et al. Semiinvasive pulmonary aspergillosis: CT and pathologic findings in six patients. *AJR Am J Roentgenol* 2000;174:795-798